J. Coord. Chem., Vol. 56, No. 9, 15 June 2003, pp. 803–816

Taylor & Francis
Taylor & Francis Group

SYNTHESIS, STRUCTURE AND PROPERTIES OF A ZINC(II) COMPLEX WITH THE LAPACHOLATE ANION AND ETHANOL AS LIGANDS

MIGUEL A. MARTÍNEZ[a,*], MARÍA C.L. DE JIMÉNEZ[a], EDUARDO E. CASTELLANO[b], OSCAR E. PIRO[c] and PEDRO J. AYMONINO[d]

[a]*Facultad de Bioquímica, Química y Farmacia, Universidad Nacional de Tucumán, Ayacucho 491, 4000 Tucumán, Argentina;* [b]*Instituto de Física de São Carlos, Universidade de São Paulo, C.P. 369, 13560 São Carlos (SP), Brazil;* [c]*IFLP-LANADI (CONICET), Departamento de Física, Facultad de Ciencias Exactas Universidad Nacional de La Plata, C.C. 67, 1900 La Plata, Argentina;* [d]*CEQUINOR and LANEFO (UNLP-CONICET), Departamento de Química, Facultad de Ciencias, Exactas, Universidad Nacional de La Plata, C.C. 962, 1900 La Plata, Argentina*

(Received 13 March 2002; Revised 3 September 2002; In final form 5 March 2003)

The reaction of lapachol, 2-hydroxy-3-(3-methyl-2-butenyl)-1,4-naphtoquinone, $C_{15}H_{14}O_3$, with zinc acetate, in ethanol, produces a chelate formula $Zn(C_{15}H_{13}O_3)_2(C_2H_6O)_2$, whose structure has been determined by single crystal X-ray diffraction. It pertains to the triclinic system, space group $P\bar{1}$ (No. 2), $a = 8.2380(3)$ Å, $b = 9.4900(2)$ Å, $c = 11.0110(4)$ Å, $\alpha = 112.536(2)^\circ$, $\beta = 91.204(2)^\circ$, $\gamma = 92.664(2)^\circ$, $Z = 1$. Some spectroscopic and chemical properties of the complex are also reported.

Keywords: Zn(II) complex; Lapacholate; Ethanol; Structure; Properties

INTRODUCTION

Lapachol (LapH) is a pigment present in the wood of some tropical plants which has been used as an antichagasic and antineoplastic agent [1]. However, it has negative effects, such as blood anticoagulation in human beings [2], and promotion of carcinogenesis in laboratory mice [3], which warn against its use as an anticancer drug. Nevertheless, pharmacologists should test complexes of the lapacholate anion (Lap) with metal cations of biological interest. In this article we report the preparation, structure and properties of a zinc(II) complex of formula: $Zn(C_{15}H_{13}O_3)_2(C_2H_6O)_2$ (for short: $Zn(Lap)_2(EtOH)_2$, the complex or **I**). $Zn(Lap)_2$ has been previously obtained electrochemically and adducts with 2,2′-bipyridine and *N*, *N*, *N*′, *N*′-tetramethylethanediamine were prepared [4].

*Corresponding author. E-mail: mamartinez@sinectis.com.ar

ISSN 0095-8972 print: ISSN 1029-0389 online © 2003 Taylor & Francis Ltd
DOI: 10.1080/0095897031000113959

EXPERIMENTAL

Preparation of the Complex

Lapachol was provided by Dr. M. Poch, Proffesor of Pharmacology, Facultad de Bioquímica, Química y Farmacia, Universidad Nacional de Tucumán, Argentina, to whom we are thankful. It was extracted with chloroform from sawdust of heart wood of Argentinian (Chaco) lapacho-trees (Tabebuia Ipé). The solid extracted was purified by recrystallization from benzene (melting range: 140–141°C; literature: 141–143°C [4]). Its infrared spectrum was identical with that reported in [5]. The complex was prepared by mixing solutions of zinc acetate dihydrate (0.03 M) and lapachol (0.06 M) in absolute ethanol, in the molar ratio 1 : 2. A dark red-brown powder precipitated from the solution and was recrystallized from the same solvent giving prismatic crystals.

Preparation of Na(Lap) · x(EtOH)

This salt was prepared (in order to compare spectral properties) by saturating 13 mL of a hot 0.1 M NaOH aqueous solution with lapachol (*ca.* 0.4 g), the excess of lapachol was separated by filtration and the solution was brought to nearly dryness (in fact, to a paste) by evaporation of water. The residue was dissolved in absolute ethanol and the solvent evaporated until dryness. Finally, the solid was washed with benzene to eliminate any unreacted lapachol.

Analyses

The lapacholate content of the complex was determined by dissolving a known amount in absolute ethanol, adding enough 0.1 N H_2SO_4 to liberate the lapachol, bringing the solution to a known volume with absolute ethanol and measuring the absorbances at 330 and 390 nm, where lapachol has absorption maxima which obey Beer's law in a wide range of concentration ($\varepsilon_{330} = 2.8 \times 10^3\,cm^{-1}\,M^{-1}$ and $\varepsilon_{390} = 1.4 \times 10^3\,cm^{-1}\,M^{-1}$) [6].

A blank test made with lapachol in the same conditions gave exactly the same absorbance values.

Ethanol content was obtained by heating at 135°C under vacuum until constant weight.

Zinc was determined chemically with zincon [7], by atomic absorption spectrophotometry performed with a Perkin Elmer A Analyst 100 spectrometer [8], from the weight of the ZnO residue left after combustion for the determination of C and H content, after heating in the samples up to 500°C in a muffle furnace in air.

The determination C and H was performed by UMYMFOR, Facultad de Ciencias Exactas y Naturales, Universidad de Buenos Aires, R. Argentina.

Solubility

The solubility in absolute ethanol was determined at room temperature by the same procedure used to determine the lapacholato content (see above) but working with a known volume of a saturated solution.

Single Crystal X-ray Diffraction

A KappaCCD X-ray diffractometer employing graphite-monochromated Mo-$K\alpha$ radiation was used. The structure was solved from 3022 reflections with intensities $I > 2\sigma(I)$ and refined by full-matrix least-squares of the nonhydrogen atoms to $R_1 = 0.046$.

Crystal data, data collection procedure, structure determination methods and refinement results are summarized in Table I. Most of the H-atoms were located among the first 20 peaks of a difference Fourier map. However, the lapacholate H-atoms were positioned stereochemically and refined with the riding model. The

TABLE I Crystal data, data collection, structure determination methods and refinement results for $Zn(Lap)_2\ (EtOH)_2$

Empirical formula	$C_{34}H_{38}O_8Zn$
Formula weight	640.02
Temperature	294(2) K
Crystal system, space group	Triclinic, $P\bar{1}$
Unit cell dimensions[a]	
	$a = 8.2380(3)$ Å
	$b = 9.4900(2)$ Å
	$c = 11.0110(4)$ Å
	$\alpha = 112.536(2)^\circ$
	$\beta = 91.204(2)^\circ$
	$\gamma = 92.664(2)^\circ$
Volume	793.53(4) Å^3
Z, Calculated density	1, 1.339 mg/m^3
Absorption coefficient	0.824 mm^{-1}
$F(000)$	336
Crystal size	$0.2 \times 0.2 \times 0.08$ mm^3
Crystal color/shape	Transparent/fragment
Diffractometer/scan	KappaCCD/ϕ and ω
Radiation, graphite monochr.	Mo-$K\alpha$, $\lambda = 0.71073$ Å
ϑ range for data collection	3.12–25.00°
Index ranges	$0 \le h \le 9$, $-11 \le k \le 11$, $-13 \le l \le 12$
Reflections collected/unique	5361/2788 [R(int) = 0.017]
Completeness to $\vartheta = 25.00^\circ$	99.8%
Max. and min. transmission	0.937 and 0.853
Observed reflections [$I > 2\sigma$(I)]	2513
Data collection	COLLECT [9]
Absorption correction	Multiscan [10]
Data reduction and correction[b]	DENZO and SCALEPACK [11]
and structure solution[c]	SHELXS-97 [12]
and refinement[d] programs	SHELXL-97 [13]
Refinement method	Full-matrix least-squares on F^2
Weights, w	$[\sigma^2 (F_o^2) + (0.0745P)^2 + 0.21P]^{-1}$
	$P = [\max(F_o^2, 0) + 2F_c^2]/3$
Data/restraints/parameters	2788/0/200
Goodness-of-fit on F^2	1.060
Final R indices[e] [$I > 2\sigma$(I)]	$R1 = 0.0410$, $wR2 = 0.1140$
R indices (all data)	$R1 = 0.0451$, $wR2 = 0.1180$
Extinction coefficient	0.032(7)
Largest diff. peak and hole	0.60 and -0.37 e·Å^{-3}

[a]Least-squares refinement of the angular settings for 20217 reflections in the $2.00 < \vartheta < 27.55^\circ$ range.
[b]Corrections: Lorentz, polarization, absorption and extinction.
[c]Neutral scattering factors and anomalous dispersion corrections.
[d]Structure solved by direct and Fourier methods. The final molecular model obtained by anisotropic full-matrix least-squares refinement of the nonhydrogen atoms.
[e]R indices defined as: $R_1 = \Sigma||F_o| - |F_c||/\Sigma|F_o|$, $wR_2 = [\Sigma w(F_o^2 - F_c^2)^2/\Sigma w(F_o^2)^2]^{1/2}$.

methyl hydrogen atoms were treated in the refinement as rigid bodies and allowed to rotate along the corresponding C–C bond such as to maximize the sum of the observed electron densities at the three calculated H-positions. The hydroxyl hydrogen atoms were refined with an isotropic displacement parameter.

Spectra

Infrared spectra were obtained from 4000 to 400 cm^{-1} with a FTIR Bruker IFS 66 instrument, and from 400 to 50 cm^{-1} with a Bruker IFS 103v apparatus; samples were recorded in KBr and polyethylene disks, respectively.

Electronic spectra (UV–Vis spectra) of ethanol solutions and KBr discs were run with a Hewlett Packard 4853 spectrophotometer.

RESULTS

Preparative

Yields of different preparations were about 70% (calculated from the amounts of lapachol used).

Physical Properties

The dark red-brown complex is stable in air and soluble in methanol, anhydrous ethanol (1.73 g/L at room temperature), ether and acetone, less soluble in benzene and carbon tetrachloride and insoluble in water.

Analytical Results

Calcd. for $C_{34}H_{38}O_8Zn$ (%): Zn, 10.2; lapacholate, 75.4; ethanol, 14.4; C, 63.8; H, 5.98. Found: Zn, 10.5 ± 0.6 (mean value of the different determinations); lapacholate, 75.2; ethanol, 13.0; C, 63.7; H, 6.08.

X-Ray Diffraction Data

The complex crystallizes in the triclinic space group $P\bar{1}$ (C_i^1, No.2), with $a = 8.2380(3)$ Å, $b = 9.4900(2)$ Å, $c = 11.0110(4)$ Å, $\alpha = 112.536(2)^\circ$, $\beta = 91.204(2)^\circ$, $\gamma = 92.664(2)^\circ$, and $Z = 1$.

Fractional coordinates and equivalent isotropic displacement parameters of the complex are given in Table II. Intramolecular bond distances and angles are presented in Table III. The anisotropic displacement parameters for heavy atoms and hydrogen coordinates and equivalent isotropic displacement parameters, respectively, are included in Tables IV and V (to be deposited). Figure 1 presents an ORTEP [14] drawing of the complex and the packing in the crystal is depicted in Fig. 2.

TABLE II Atomic fractional coordinates and equivalent isotropic displacement parameters for $Zn(Lap)_2$ $(EtOH)_2$

Atom	*x*	*y*	*z*	U_{eq}
Zn	10000	0	10000	57(1)
O(1)	8355(2)	−1974(2)	8902(2)	58(1)
O(2)	10022(2)	−1162(2)	11170(2)	53(1)
O(3)	8177(2)	−5763(2)	11439(2)	59(1)
O(4)	7964(3)	1236(2)	10972(3)	93(1)
C(1)	8263(3)	−2864(2)	9467(2)	44(1)
C(2)	7254(3)	−4305(2)	8919(2)	45(1)
C(3)	6343(3)	−4685(3)	7757(3)	58(1)
C(4)	5417(3)	−6047(3)	7246(3)	67(1)
C(5)	5406(3)	−7028(3)	7905(3)	66(1)
C(6)	6309(3)	−6660(3)	9068(3)	56(1)
C(7)	7237(3)	−5285(2)	9598(2)	44(1)
C(8)	8182(3)	−4850(2)	10878(2)	44(1)
C(9)	9078(3)	−3391(2)	11448(2)	42(1)
C(10)	9182(3)	−2436(2)	10766(2)	42(1)
C(11)	9915(3)	−2925(3)	12776(2)	49(1)
C(12)	8933(3)	−1856(3)	13835(2)	53(1)
C(13)	8291(3)	−2060(4)	14843(3)	65(1)
C(14)	7330(5)	−868(5)	15810(4)	104(2)
C(15)	8415(7)	−3489(6)	15109(4)	112(2)
C(16)	6840(6)	1000(5)	11864(5)	108(2)
C(17)	7330(11)	1912(8)	13193(7)	186(3)

TABLE III Interatomic bond distances and angles in $Zn(Lap)_2(EtOH)_2$[a]

Bond distances	
Zn–O(2)	1.991(2)
Zn–O(4)	2.152(2)
Zn–O(1)	2.183(2)
O(1)–C(1)	1.226(3)
O(2)–C(10)	1.279(3)
O(3)–C(8)	1.243(3)
O(4)–C(16)	1.436(4)
C(1)–C(2)	1.472(3)
C(1)–C(10)	1.505(3)
C(2)–C(3)	1.383(4)
C(2)–C(7)	1.399(3)
C(3)–C(4)	1.379(4)
C(4)–C(5)	1.382(5)
C(5)–C(6)	1.381(4)
C(6)–C(7)	1.390(3)
C(7)–C(8)	1.497(3)
C(8)–C(9)	1.440(3)
C(9)–C(10)	1.382(3)
C(9)–C(11)	1.497(3)
C(11)–C(12)	1.501(3)
C(12)–C(13)	1.314(4)
C(13)–C(14)	1.495(4)
C(13)–C(15)	1.500(5)
C(16)–C(17)	1.423(8)
Bond angles	
O(2′)–Zn–O(4)	88.47(8)
O(2)–Zn–O(4)	91.53(8)
O(2′)–Zn–O(1)	101.50(6)

(*continued*)

TABLE III Continued

Bond distances	
O(2)–Zn–O(1)	78.50(6)
O(4)–Zn–O(1)	89.89(9)
O(4′)–Zn–O(1)	90.11(9)
C(1)–O(1)–Zn	110.6(2)
C(10)–O(2)–Zn	116.6(2)
C(16)–O(4)–Zn	132.3(2)
O(1)–C(1)–C(2)	121.6(2)
O(1)–C(1)–C(10)	118.5(2)
C(2)–C(1)–C(10)	119.9(2)
C(3)–C(2)–C(7)	120.6(2)
C(3)–C(2)–C(1)	120.8(2)
C(7)–C(2)–C(1)	118.6(2)
C(4)–C(3)–C(2)	120.2(3)
C(3)–C(4)–C(5)	119.5(3)
C(4)–C(5)–C(6)	120.8(2)
C(5)–C(6)–C(7)	120.3(2)
C(6)–C(7)–C(2)	118.6(2)
C(6)–C(7)–C(8)	120.9(2)
C(2)–C(7)–C(8)	120.5(2)
O(3)–C(8)–C(9)	120.7(2)
O(3)–C(8)–C(7)	119.0(2)
C(9)–C(8)–C(7)	120.3(2)
C(10)–C(9)–C(8)	120.2(2)
C(10)–C(9)–C(11)	120.2(2)
C(8)–C(9)–C(11)	119.6(2)
O(2)–C(10)–C(9)	124.1(2)
O(2)–C(10)–C(1)	115.7(2)
C(9)–C(10)–C(1)	120.2(2)
C(9)–C(11)–C(12)	111.5(2)
C(13)–C(12)–C(11)	128.6(3)
C(12)–C(13)–C(14)	121.6(3)
C(12)–C(13)–C(15)	123.9(3)
C(14)–C(13)–C(15)	114.5(3)
C(17)–C(16)–O(4)	111.0(5)

[a]Primed atoms are obtained from the unprimed ones through the inversion symmetry operation: $-x+2$, $-y$, $-z+2$.

Spectra

Figure 3 reproduces the infrared spectrum of Complex (**I**) from 4000 to 50 cm^{-1}, which is the result of joining automatically the partial spectra run with the two Bruker instruments (from 4000 to 400 cm^{-1} with the IFS 66 and from 400 to 50 cm^{-1} with the IFS 113v). Figure 4 shows the electronic spectra of the complex as a solid in a KBr disk (a) and in a 4.64×10^{-6} M solution in absolute ethanol (b).

DISCUSSION

Structure

Bond distances and angles presented in Table III agree very well with those reported for the lapacholate anion in the complex; $Cu(Lap)_2(bpy)_2$ [5] and also, with values corresponding to the two forms (I, triclinic and II, monoclinic) of lapachol, as far as they can be compared because the protonation of lapachol [15].

TABLE IV Anisotropic displacement parameters for heavy atoms of $Zn(Lap)_2(EtOH)_2$

Atom	U_{11}	U_{22}	U_{33}	U_{23}	U_{13}	U_{12}
Zn	84(1)	35(1)	58(1)	26(1)	7(1)	−8(1)
O(1)	86(1)	43(1)	52(1)	28(1)	−3(1)	−7(1)
O(2)	75(1)	37(1)	51(1)	22(1)	−3(1)	−13(1)
O(3)	86(1)	40(1)	63(1)	31(1)	14(1)	1(1)
O(4)	123(2)	50(1)	123(2)	50(1)	61(2)	18(1)
C(1)	56(1)	35(1)	45(1)	19(1)	8(1)	2(1)
C(2)	49(1)	38(1)	46(1)	15(1)	7(1)	1(1)
C(3)	64(1)	57(1)	54(1)	23(1)	0(1)	−2(1)
C(4)	59(1)	68(2)	62(2)	12(1)	−7(1)	−11(1)
C(5)	58(1)	49(1)	77(2)	12(1)	6(1)	−12(1)
C(6)	58(1)	39(1)	69(2)	19(1)	14(1)	−6(1)
C(7)	47(1)	34(1)	52(1)	16(1)	13(1)	2(1)
C(8)	52(1)	34(1)	51(1)	21(1)	16(1)	6(1)
C(9)	50(1)	36(1)	45(1)	19(1)	11(1)	5(1)
C(10)	52(1)	31(1)	44(1)	17(1)	8(1)	1(1)
C(11)	58(1)	48(1)	47(1)	24(1)	5(1)	3(1)
C(12)	63(1)	46(1)	46(1)	15(1)	0(1)	−1(1)
C(13)	65(2)	76(2)	45(1)	13(1)	4(1)	−10(1)
C(14)	87(2)	124(3)	61(2)	−9(2)	19(2)	−3(2)
C(15)	150(4)	126(4)	82(3)	65(3)	23(3)	−6(3)
C(16)	146(4)	73(2)	127(4)	58(2)	65(3)	23(2)
C(17)	276(10)	154(6)	142(6)	75(5)	46(7)	−7(6)

TABLE V Hydrogen coordinates and equivalent isotropic displacement parameters for $Zn(Lap)_2(EtOH)_2$

Atom	*x*	*y*	*z*	U_{eq}
H(3)	6354	−4019	7318	70
H(4)	4804	−6303	6464	81
H(5)	4783	−7948	7561	79
H(6)	6295	−7334	9498	67
H(11A)	10970	−2428	12774	59
H(11B)	10088	−3828	12961	59
H(12)	8754	−927	13770	63
H(14A)	7922	−443	16643	156
H(14B)	6304	−1322	15913	156
H(14C)	7149	−73	15494	156
H(15A)	7343	−3913	15140	168
H(15B)	8993	−3250	15936	168
H(15C)	8989	−4219	14419	168
H(16A)	5765	1259	11674	130
H(16B)	6781	−70	11741	130
H(17A)	6578	1713	13771	278
H(17B)	7342	2973	13325	278
H(17C)	8399	1664	13379	278
H	8139	2154	11027	82(10)

The zinc(II) ion is at a crystallographic inversion center in a slightly tetragonally distorted octahedral environment, equatorially coordinated to two symmetrically related lapacholate anions acting as bidentate ligands through their carbonyl and phenolic oxygen atoms (Zn–O distances are 2.183(2) and 1.991(2) Å, respectively) and axially to two ethanol molecules through the hydroxyl oxygen atoms (d(Zn–O) = 2.153(2) Å). O–Zn–O (*cis*) angles in the ZnO_6 core are in the range from 78.45(6) to 101.55(6)°.

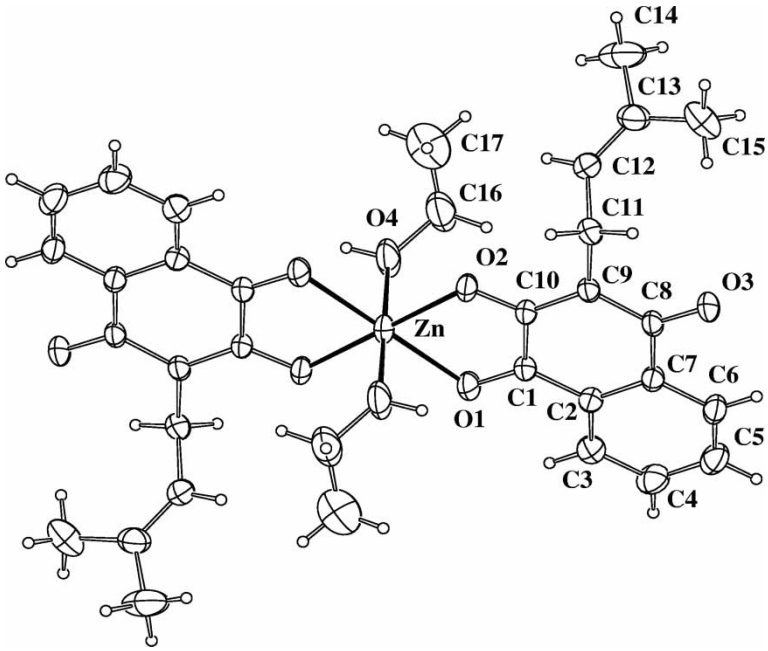

FIGURE 1 ORTEP drawing of the molecular structure of $Zn(Lap)_2(EtOH)_2$ with the numbering and displacement ellipsoids (at 30% probability level) of nonH-atoms.

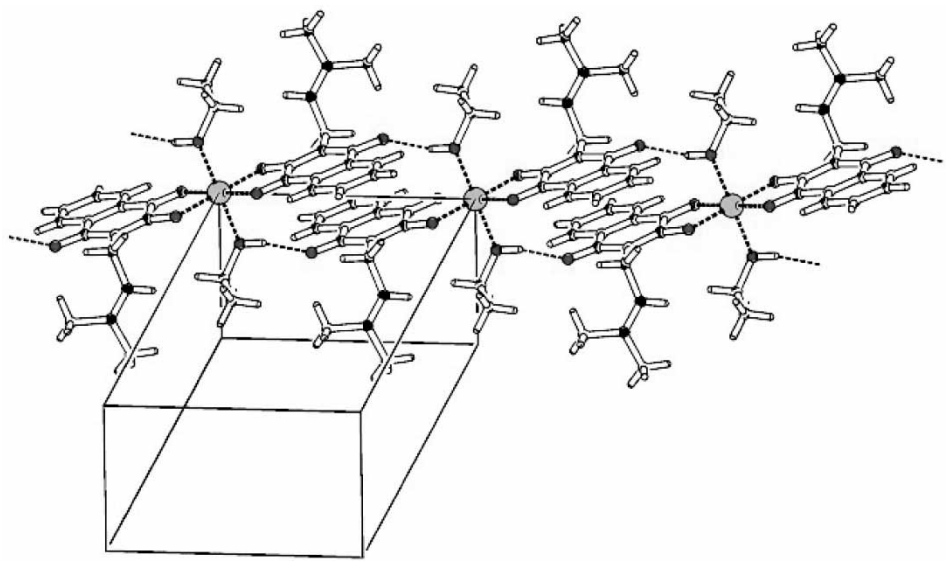

FIGURE 2 Crystal packing for $Zn(Lap)_2(EtOH)_2$.

In $Cu(Lap)_2bpy$ [5] the equatorial plane of the tetragonally, Jahn-Teller distorted coordination octahedron, is defined by the bpy nitrogen atoms and the phenolic oxygen atom of each lapacholate anion (*d*(Cu–O): 1.950(6), 1.923(6) Å) (the CuN_2O_2 moiety is planar within 0.054 Å) while the apical positions (orthogonal to the equatorial

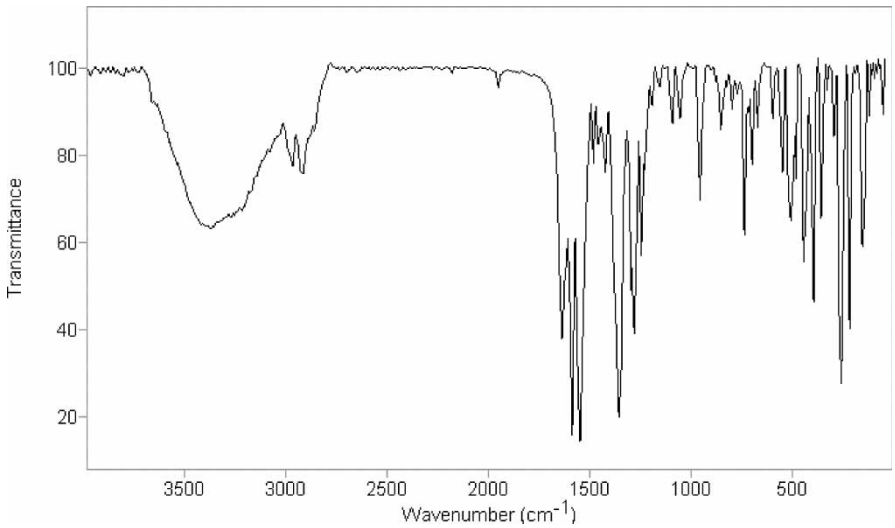

FIGURE 3 Infrared spectrum of $Zn(Lap)_2(EtOH)_2$.

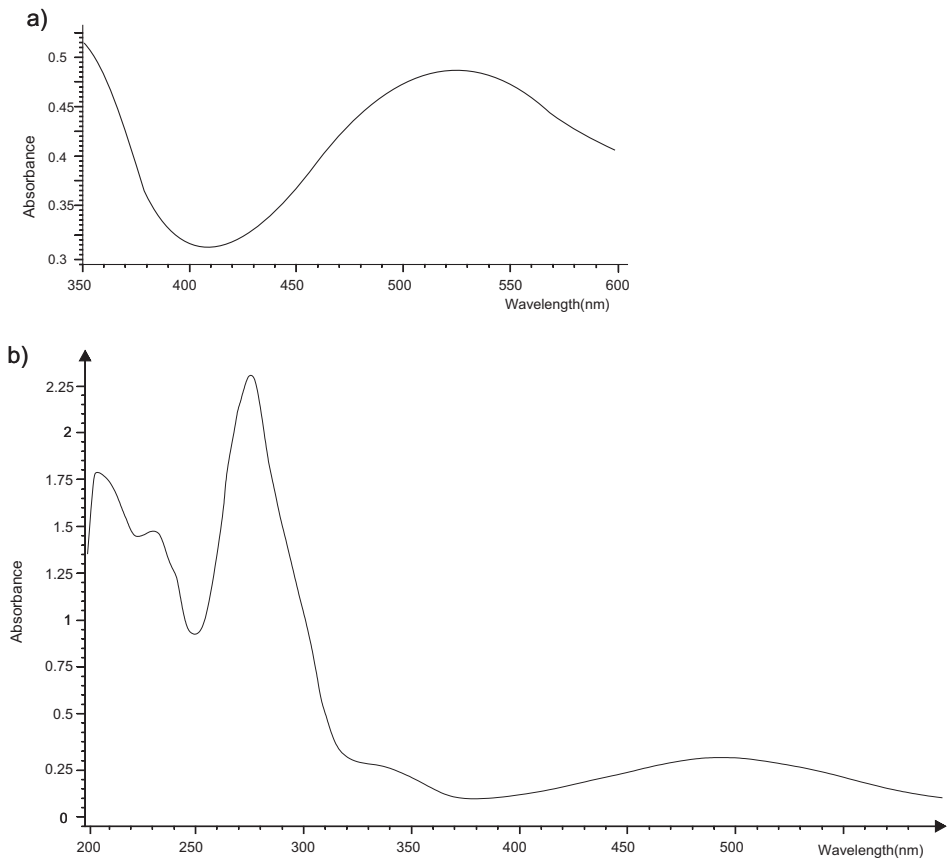

FIGURE 4 Electronic spectra of $Zn(Lap)_2(EtOH)_2$ as a solid (a) and in a 4.64×10^{-5} M solution in absolute ethanol (b).

plane) are occupied by the carbonyl oxygen atoms neighboring to the phenolic groups (d(Cu–O): 2.40(1), 2.44(1)Å). The lapacholate rings are, therefore, normal to the equatorial plane.

The two naphthoquinone rings in the complex are nearly planar; the r.m.s. deviation of atoms from the least-square plane is 0.051 Å. The Zn(II) ion departs 0.119(2) Å from this plane and the ethanol oxygen atoms are 2.027(3) each from the nearest planes. The butenyl lateral chains are planar within experimental accuracy (r.m.s deviation: 0.0041 Å) and the planes form a $70.21 \pm 0.08^\circ$ dihedral angle with the naphthoquinone planes. In lapachol the two planes are nearly perpendicular to each other (84.6(2)/87.7(4)°, dihedral angle for forms I and II, respectively) [15]. This fact has been explained by the presence of weak interactions between C11–H11A···O2 and C11–H11B···O4 [15].

It is to be noted that the C10–O2 and C8–C9 bonds lengths (1.279 and 1.440 Å, respectively) are shorter than in lapachol [15] (1.347/1.350 Å, in I and II forms, and 1.478/1.471 Å, respectively) and the C9–C10 distance (1.382 Å) is either larger or equal to the same distance in lapachol (1.352/1.382 Å), and the C8–O3 bond length (1.243 Å) is also larger than in lapachol (1.225/1.232 Å). These facts could be explained by resonance (mesomerism) between O2 and O3 (between the *para*- and *ortho*-naphthoquinone forms, respectively) which in lapachol is more restricted because of the protonation of O2 (for the enhancement of the mesomerism by intermolecular H-bonding see below). In fact, the H–O2–C10=C9–C8=O3 tautomer is considered to be about 43 kJ mol^{-1} more stable than the O2=C10–C9=C8–O3–H tautomer in lawsone (2-hydroxy-1,4-naphthoquinone) [16].

It is also interesting to compare some bond distances between the complex and Cu(Lap)$_2$(bpy)$_2$, i.e., Zn–O2 (phenolic): 1.991 Å, Cu–O2 (O1 and O5 in [4]): 1.950/1.923 Å; Zn–O1(carbonylic): 2.184 Å, Cu–O1 (O2 and O4): 2.40/2.44 Å. The M–O(phenolic) distance is greater for Zn than for Cu (difference: 0.041/0.068 Å), in accordance with the difference in the M(II) ionic radii predicted by linear interpolation between Ni(II) and Zn(II) radii (see, for instance [17], but if the Jahn-Teller effect (of which Cu(II) is paradigmatic) is taken into account, the relative values of M(II) radii are inverted because Zn(II) size turns out to be smaller than that of Cu(II) (difference in Goldschmidt radii: −0.03 Å [17]). This fact is reflected in the M–O (axial) distances, which in the Zn complex are 2.153(2) Å and in the Cu complex, 2.40/2.44 Å.

As shown in Fig. 2, the Zn(Lap)$_2$ groups are located in parallel sheets, as in lapachol [15], displaced by a unit cell translation along the b-axis. Anyway, each naphthoquinone group has, as neighbor, a similar group above or below it, at an interplanar distance of 3.08(3) Å. This separation is small enough to allow π–π^* interactions between the naphthoquinone rings, as suggested for lapachol, in which crystals of both varieties (I and II) had rings in parallel and partially superimposed [15] and at 3.29/3.75 Å distance from each other. But the components of the crystal (the complexes) are not only bonded together by such interactions and van der Waals forces but also by intermolecular O–H···O bridges spanning between the ethanol hydroxyl groups (HO4) of each complex and the nonbonded-to-metal oxygen atoms (O3′) of neighboring complexes (d(H···O3′) = 1.849 Å, ∠ (O4–H···O3′) = 167°), as shown in Fig. 2. In lapachol, there are dimers in which the monomers are joined by pairs of O–H···O bridges spanning between the HO phenolic group of one of the components and the o-O(quinonic) atom of the other [15].

IR Spectrum

The infrared spectrum of Complex (**I**) (Fig. 3) up to 666 cm^{-1} is quite comparable, to the features assignable to the anion, with the spectrum of the complex salt said to be $Fe(Lap)_2$ (**II**) [5].

It is also interesting to compare with the spectrum of $Na(Lap) \cdot x(EtOH)$ (**III**).

In the region of the HO stretch of **I** there are two main features, i.e.: a very weak but well-defined shoulder at 3655 cm^{-1}, which can be assigned to free (not hydrogen-bonded) hydroxyls, laying at the surface of the very fine grains produced by grinding the sample in an agate mortar to prepare the KBr disks. The other feature is a broad band centered at about 3367 cm^{-1} due to the HO groups involved in intermolecular hydrogen-bonds. Obviously, the spectrum of **II** does not show such bands while in the spectrum of **III** there is also a broad band centered at *ca.* 3390 cm^{-1}. It is to be noted that hexaethanol complexes of magnesium, calcium and first series transition metal divalent cations show the broad band assigned to the HO stretches between 3490 and 3300 cm^{-1}, depending on the coordinative capacities of the (counter)anions ($BF_4^- < ClO_4^- < NO_3^-$) [18].

The lapachol (**IV**) spectrum shows a very strong but rather narrow and sharp HO (phenolic), H-bonded stretching band at 3354 cm^{-1}. Bands of **I** at 2962 and 2916 cm^{-1} are due to CH stretches, which in the **III** and **IV** spectra appear at 2966 and 2916, and 2971 and 2908 cm^{-1}, respectively, with the same relative intensities, in the three cases. Bands seen at 1662 and 1641 cm^{-1} (our values) in the **IV** spectrum have been assigned to the carbonyl groups [5]. The band at 1593 cm^{-1} should be assigned to a ring mode (see below) [19]. When **IV** is deprotonated, as it is in the sodium salt (**III**), those bands shift to 1666 and 1527 cm^{-1} and the second seems to gain intensity in comparison with the first (the ring band is located at 1591 cm^{-1}, only -2 cm^{-1} from the corresponding band in **IV**). The respective shifts could be explained if the band of highest wavenumber is assigned to the C1O1 group, which slightly shifts towards NIR ($+4$ cm^{-1}) due to the rupture of the dimers of lapachol and therefore, of the C1O1$\cdots$H′O2′ hydrogen bonds, with the increase of the CO stretching wavenumber. On the contrary, in **I**, this band moves towards FIR (1635 cm^{-1}, shift: -27 cm^{-1}) because of the coordination with Zn(II), which brings about a reduction of the bond order. The other band should have a much greater shift, also in the FIR direction, because the resonance $^-$O2–C10=C9–C8=O3$\leftrightarrow$O2=C10–C9=C8–O3$^-$ which brings about a reduction of the bond order of the C8O3 group by the mesomerism with the phenolate group. The shift for **III** is -114 cm^{-1} and **I**, -94 cm^{-1}. The difference between those figures should be ascribed to the net negative charge present in **III** which is partially compensated in **I** by coordination to Zn(II). These assignments are in accord with the respective C–O distances in **I**, which are 1.226 and 1.242 Å, for C10O2 and C8O3, respectively. This criterion is not useful in the case of **IV** because with respective bond lengths of 1.225(I)/1.237(II) Å and 1.225/1.232(II) Å [15], the prediction would be: $\tilde{\nu}$C1O1 $\leq \tilde{\nu}$C8O3. For lawsone [16], instead of individual C=O stretches, coupled asymmetric and symmetric vibrations are proposed, which are assigned to a very weak band at 1710 cm^{-1} (Ar-matrix)/ 1711 cm^{-1} (N_2-matrix) and to a very strong band at 1673/1679 cm^{-1} (see the spectrum of the solid [5]), a -136 cm^{-1} (single) shift is reported for the carbonyl peaks [5], not far from the -124 cm^{-1} value reported above for **I**, while for $Fe(lawsone)_2$, downshifts are only 76 and 52 cm^{-1} (from 1681 to 1631 cm^{-1}, in lawsone, respectively). The strongest

peak at 1655 cm^{-1} in the spectrum of $Ni(Lap)_2 \cdot 2.5H_2O$ (**V**) [20], assigned to a carbonyl stretch, is shifted towards FIR showing the participation of the group in complexation.

It is to be noted that the wavenumbers of the band which appears in the C=O stretching region of the spectra of **I**, **III** and **IV** (see above) does not differ much among the different naphthoquinonic spectra; so, in the 1,4-naphthoquinone spectrum it is at 1585 cm^{-1} [21], in lawsone, at 1603 cm^{-1} (the same in Ar- and N_2-matrices) [16]; while in **I** it is at 1587 cm^{-1}; in **III** at 1591 cm^{-1} and in **IV** at 1593 cm^{-1}.

The C10–O2 (single bond, phenolic) stretching band in **IV** should be between 1260 and 1180 cm^{-1} [20] but in matrix-isolated lawsone [16] this vibration contributes to bands at 1394/1395 cm^{-1} (Ar–N_2 matrices), 1306/1307 cm^{-1}, 1215/1218 cm^{-1} and 990/990 cm^{-1}. In all cases, the contribution of ν(C10O2) to the potential energy distribution is less than 20%. Therefore, it seems impossible to assign a single band to that vibration. The absence in **III** and **I** spectra of the medium strong band present at 1311 cm^{-1} in **IV** (the apparent intensity of this band is increased by the neighboring, very strong bands that flank it at 1369–1344 (a complex band) and 1273 cm^{-1}). In those spectra, this bands could be NIR shifted and hidden under the very strong bands located at 1375 and 1354 cm^{-1}, respectively. The shifts could be due to the lack in **III** and **I** of the O2H···O1′ intermolecular bonding in the dimers present in **IV** and the coupling of $C10O2^{x-}$ ($x = 1$ in **III**; $x \ll 1$ in **I**) with C8O3, in any case more effective than in **IV**.

For further assignments of bands to the lawsone moiety of lapachol [16] to the lateral chain [22] have been reported.

The Zn-O stretches of the *pseudo*-octahedral coordination polyhedron should be expected in the region ranging from 500 to 200 cm^{-1} because the Cu^{2+} and Ni^{2+} acetylacetonates ($M(acac)_2$)) have such bands at 455 and 291 cm^{-1}, and 438 and 271 cm^{-1}, respectively [23], while for $[Zn(H_2O)_6]SO_4 \cdot H_2O$ a band at 364 cm^{-1} has been assigned to that vibration [23] and in $Ca(EtOH)_4Br_2$ this band is at 320 cm^{-1} [24]. In that region of the spectrum of **I** there are weak bands at 480, 357 and 293 cm^{-1} which do not appear in the spectrum of **III** and could be assigned to the Zn–O stretchings.

Electronic Spectra

As shown in Fig. 4(a), in the visible region, the spectrum of the solid presents a strong broad absorption band centered at 520 nm, responsible for the characteristic strong red-brown color. This color should be compared with the yellow color of lapachol, in which the corresponding band is blue-shifted to 430 nm. This band could be assigned to a $n \rightarrow \pi^*$ transition the quinone carbonyls [25]. In **I** the mesomerism between C10O2 and C8O3, favored in the solid by the O3···HOEt bridges, should be the phenomenon responsible for the bathochromic shift of this band with respect to lapachol. In absolute ethanol solution of **I** (see Fig. 4b), this band shifts to 496 nm, a fact that could be due to EtOH(solvent)–π interactions (which replace the π–π^* interactions between neighboring rings in the solid). It is interesting that in ethanolic solutions, the band of **IV** in the visible shifts to 490 nm, which has been attributed to the $^-$O2–C10=C9–C8=O3$\leftrightarrow$O2=C10–C9=C8–$O3^-$ mesomerism (*p*-quinone $\leftrightarrow$ *o*-quinone) [26]. Actually, what really seems to happen is that protonation of O2 fixes the first form while deprotonation gives place to the mesomerism between the two forms. Bands assignable to $\pi \rightarrow \pi^*$ transitions in the aromatic rings are at 214 and 231 nm (benzene ring), 277 nm (quinonic ring) and 340 nm (benzene ring) [25].

CONCLUSIONS

The reaction of zinc acetate and lapachol in absolute ethanol produces a complex salt of formula: $Zn(Lap)_2(EtOH)_2$, in which the oxygen atoms of the ligands are coordinated to the Zn(II) ion in a nearly octahedral configuration. The lapacholate anions (Lap) act as bidentate ligands bonded to the zinc ion through oxygen atoms of the phenolic group and of the adjacent quinonic carbonyl, which define the equatorial plane of the octahedron, while the poles are occupied by the oxygen atoms of the ethanol molecules. Zn(II) is located in the center of the coordination polyhedron, which is an inversion center. In the solid, individual complexes are joined together in chains by intermolecular hydrogen bridges formed between the ethanolic hydrogen atoms of one molecule and the *p*-quinonic oxygen atoms of neighboring complexes. Some $\pi \rightarrow \pi^*$ interactions exist between adjacent naphthoquinonic rings of neighboring chains. The hydrogen bridges generate an IR broad and strong absorption band centered at 3400 cm^{-1}. Its position suggests that those bridges are rather strong.

The strong red-brown color of the solid complex is due to a broad and strong band centered at 520 nm in the visible spectrum, which could be assigned to mesomerism in the conjugated system of the quinonic ring of the anion: $^{-}$O2–C10=C9–C8=O3 $\leftrightarrow$ O2=C10–C9=C8–O3^{-} (*p*-quinone $\leftrightarrow$ *o*-quinone). The slight change of color which occurs when the solid is dissolved in absolute ethanol (maximum absortion at 496 nm) could be due to breaking of the $\pi \rightarrow \pi^*$ interaction between adjacent naphthoquinonic rings and replacement by EtOH$\cdots\pi$ interactions.

Acknowledgments

To CONICET, ANPCyT, CICPBA, UNLP, CIUNT and UNT, R. Argentina and to FAPESP and CNPq of Brazil for financial help.

Supplementary Material

Tables containing anisotropic parameters and hydrogen coordinates and equivalent isotropic displacement parameters have been deposited in the Cambridge Crystallographic Data Centre as supplementary publication CCDC. Copies can be obtained, free of charge, on application to the Director, CCDC, 12, Union Road Cambridge CB2 1EZ, UK (Fax: +44-(0)1223-336033 or E-mail: deposit@chemcrys.cam.ac.uk).

References

[1] K.V. Rao, T.J. Mc Bride and J.J. Olenson, *Cancer Res.* **28**, 1952 (1968).
[2] J.B. Block, A.A. Serpick, W. Miller and P.H. Wiernick, *Cancer Chemother. Rep.* Part 2, **4**, 27 (1974).
[3] N.A. de Sandoval, C.P. Rodriguez and N.R. de Martínez, *Acta Phisiol Pharmacol Ther Latinoam.* **46**(4), 257–264 (1996).
[4] E.H. de Oliveira, G.A. Medeiros, C. Peppe, M.A. Brown and D.G. Tuck, *Can. J. Chem.* **75**, 499 (1997).
[5] A. Dufresne, C.G. de Lima, J. Knudsen and J.E. Moreira, *J. Inorg. Nucl. Chem.* **35**, 789 (1973).
[6] S. da Guia Mello Portugal, J.O. Machuca Herrera and I.M. Brinn, *Bull. Chem.Soc. Jpn.* **70**, 2071 (1997).
[7] F.D. Snell, C.T. Snell and C.A. Snell, Colorimetric Methods of Analysis, Vol II A (D. van Nostrand Co., New Jersey, 1959), p. 317.
[8] Perkin Elmer, Analytical Methods for Atomic Absorption Spectrometry (The Perkin Elmer Corporation, USA, 1994), p. 125.

[9] Enraf-Nonius. Collect. Nonius BV (Delft, The Netherlands 1997–2000).
[10] R.H. Blessing, *Acta Cryst*. **A51**, 33 (1995).
[11] Z. Otwinowski and W. Minor, In: C.W. Carter, Jr. and R.M. Sweet (Eds.), Methods in Enzymology, Vol. 276. (Academic Press, New York, 1997), pp. 307–326.
[12] G.M. Sheldrick, SHELXS-97, Program for Crystal Structure Resolutioni (University of Göttingen, Göttingen, Germany, 1997).
[13] G.M. Sheldrick, SHELXL-97, Program for Crystal Structures Analysis (University of Göttingen: Göttingen, Germany, 1997).
[14] C.K. Johnson, ORTEP-II: A Fortran Thermal-Ellipsoid Plot Program. Report ORNL-5138 (Oak Ridge National Laboratory, Tennessee, USA, 1976).
[15] I.K. Larsen, L.A. Andersen and B.F. Pedersen, *Acta Cryst*. **C48**, 2009 (1992).
[16] H. Rostkowskam, M.J. Nowak, L. Lapinski and L. Adamowicz, *Spectrochim. Acta* **A54**, 1091 (1998).
[17] F.A. Cotton and G. Wilkinson, Advanced Inorganic Chemistry, 4th Edn. (J. Wiley and Sons, New York, 1980), p. 678.
[18] P.W.N.M. van Leeeuwen, *Rec. Trav. Chim*. **86**, 247 (1967).
[19] E. Pretsch, J. Seibl, W. Simon and Th. Clerc, Spectral Data for Structure Determination of Organic Compounds, 2nd Edn. (Springer Verlag, Berlin-Heidelberg, 1989).
[20] S.S. Sawhney and S.D. Matta, *J. Indian. Chem. Soc*. **LVII**, 497 (1980).
[21] B. Schrader, Raman/Infrared Atlas of Organic Compounds. 2nd edn (VCH Verlagsgesselschaft m.b.H., Weinheim, 1989).
[22] J. Peng, N. Mina-Camilde, and I.C. Manzanares, *Vibrat. Spectrosc*. **8**, 319 (1995).
[23] K. Nakamoto, Infrared and Raman Spectra of Inorganic and Coordination Compounds, Part B. 5th Edn. (John Wiley & Sons, Inc., New York, 1997).
[24] S. Halut-Desportes and E. Husson, *Spectrochim. Acta* **41A**, 661 (1985).
[25] I. Sing, R.T. Ogata, R.E. Moore, C.W.J. Chang and P.J. Scheuer, *Tetrahedron* **24**, 6053 (1968).
[26] S.S. Sawhney and (KM.) N. Vohra, *J. Indian. Chem. Soc*. **LIV**, 403 (1977).